Discotic charge transfer twins Structure and mesophase behaviour of covalently linked triphenylenes and trinitrofluorenones

M. Möller[a]; V. Tsukruk[ab]; J. H. Wendorff[a]; H. Bengs[c]; H. Ringsdorf[c]

[a] Deutsches Kunststoff Institut, Darmstadt, Germany [b] Institute of Bioorganic Chemistry, Academy of Science of Ukraine, Kiev, Ukraine [c] Universität Mainz, Institut für Organische Chemie, Mainz, Germany

PLEASE SCROLL DOWN FOR ARTICLE

Discotic charge transfer twins

Structure and mesophase behaviour of covalently linked triphenylenes and trinitrofluorenones

by M. MÖLLER, V. TSUKRUK† and J. H. WENDORFF*

Deutsches Kunststoff Institut, Schloßgartenstr. 6,
6100 Darmstadt, Germany

H. BENGS and H. RINGSDORF

Universität Mainz, Institut für Organische Chemie,
J. J. Becher-Weg 18–20, 6500 Mainz, Germany

Discotic charge transfer twins, a novel class of discotic liquid-crystalline compounds were studied. These compounds consist of triphenylene units (as donors) which are chemically linked via flexible spacers of various lengths to trinitrofluorenone units (acting as acceptor). They display a liquid-crystalline phase over a wide temperature range extending up to 240–260°C. Based on X-ray analysis a structural model is proposed for the liquid-crystalline phase: the molecules are arranged in columns in such a way that mixed stacks occur, the intercolumnar packing possesses an orthorhombic symmetry. The neighbouring columns are connected along specific directions via flexible spacers which give rise to highly anisotropic structural properties of this columnar liquid-crystalline phase.

1. Introduction

Organic compounds able to self-organize are of increasing interest because of their special physical properties such as electrical conductivity [1–3], superconductivity [4] or non-linear optical properties [5]. They may serve therefore, in many cases as substitutes for inorganic materials. Liquid crystals built from form-anisotropic molecules belong to this category. They are able to form supramolecular structures leading to anisotropic materials with direction dependent physical properties. It is for this reason that molecular engineering of organic compounds including monomeric and polymeric liquid crystals and their functionalization is currently a very active area [6–8].

The combination of different structural elements in a single molecule very often leads to unexpected supramolecular structures: the combination of rod-shaped and disc-shaped molecules based on azobenzenes and triphenylenes, for instance, has led to liquid-crystalline materials of a wall-type structure with segregated columns [9]. Another possibility consists in functionalizing liquid crystals with second components in a mixture [10–19]. Examples are discotic systems doped with inorganic materials such as iodine, bromine or aluminium chloride [10–12] which become conducting. A

drawback of this approach is that the choice of the molar ratio is very critical. The phase width is decreased or the phase structure may even be lost by the mixing process. One way to overcome this problem is to prepare mixtures with non-discoid, but flat, organic molecules, giving rise to additional interactions with the phase forming system such as charge transfer interactions [13,14]. In ideal cases, for example disc-like electron rich triphenylenes and electron poor molecules (such as 2,4,7-trinitrofluoren-one=TNF), this may not only lead to functionalized phases with a broadened phase width but also to phase induction in discoid, but non-liquid-crystalline systems [15–17] (see figure 1). Simple physical mixing, nevertheless, may give rise to phase separation of the donor and acceptor units at higher concentrations of the non-discoid compound [15]. It was of interest, therefore, to study systems where the function and phase forming moiety are directly coupled to each other chemically. Such an approach will be described in this paper. The coupling of electron rich triphenylenes and electron poor trinitrofluorenones via flexible spacers of different length leads to the twin molecules 1 and 2 (scheme 1). The synthesis, structure and phase behaviour of these novel liquid-crystalline compounds will be described.

Scheme 1.

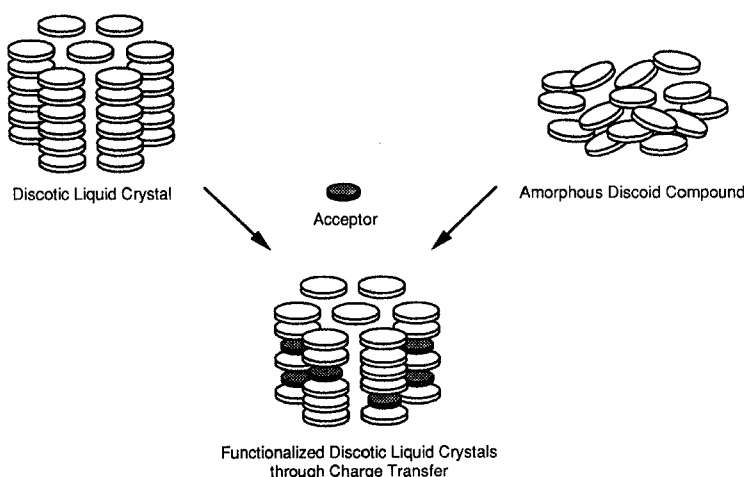Functionalized Discotic Liquid Crystals
through Charge Transfer
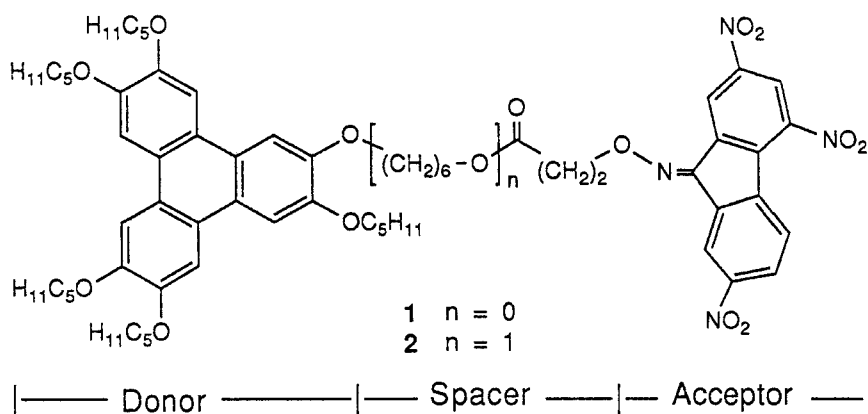
Figure 1. Schematic representation of functionalized discotic liquid crystals: variation (left) and induction (right) of liquid-crystalline phases in disc-shaped donors by mixing with acceptors (for the sake of clarity donors are drawn without side chains).

2. Experimental procedures

2.1. *Preparation of the samples*

The synthesis of the samples is presented in scheme 2.
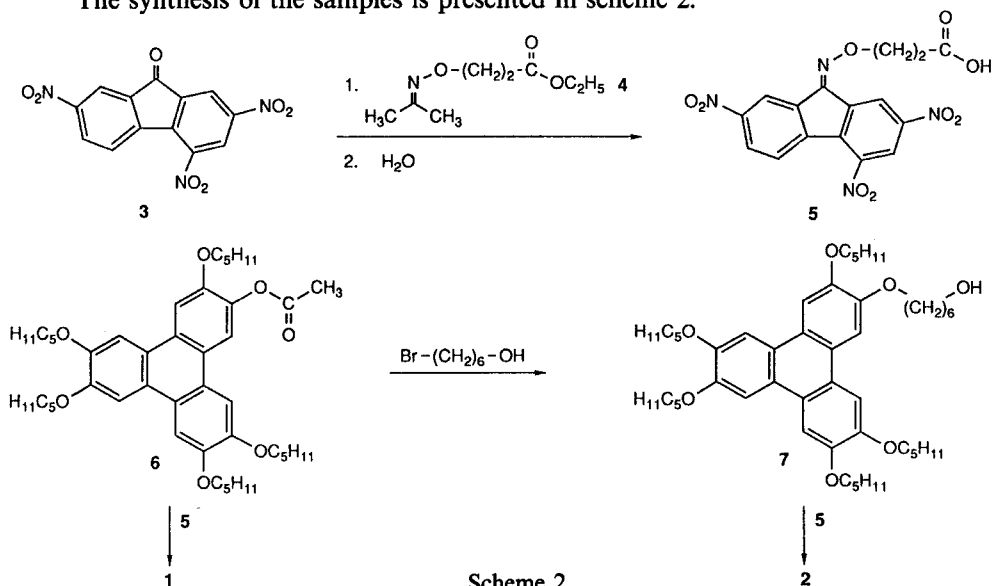
Scheme 2.

2.1.1. *β-(2,4,7-Trinitro-9-fluorenylideneaminooxy) propionic acid* 5

The synthesis of this compound was performed according to the literature [20, 21], using 40 g (102 mmol) of TNF 3 (80 per cent, Janssen Chimica) and 18 g (104 mmol) of the alkylated oxime 4 [20] in 400 ml of acetic acid with 3 g (15·8 mmol) of 4-toluenesulfonic acid monohydrate as catalyst. Hydrolysis of the corresponding ester and twofold recrystallisation from acetone yielded 35 g (86 per cent) of bright yellow crystals. Mp = 202–6°C. IR(KBr): $\tilde{v}$ = 1700 cm^{-1} (C=O). ^{1}H NMR (400 MHz, acetone-d_6): δ (ppm) = 9·34 and 9·11 (2s; 1 H, H^3), 8·95 and 8·88 (2s, 1 H, H^1), 8·70 and 8·58 (2s, 1 H, H^8), 8·54 and 8·43 (2d, 1 H, H^6), 8·28 and 8·18 (2d, 1 H, H^5), 4·90 (t; 2 H, N–O–CH$_2$), 3·02 (t; 2 H, CH$_2$–CO–OH). MS (EI): m/e (per cent) = 402 (M$^+$, 16), 330 (=N–O–H$^+$, 67), 314 (=N–H$^+$, 100). UV-Vis(Acetonitrile): λ_{max}/nm (log ε) = 282 (4·6). C$_{16}$H$_{10}$N$_4$O$_9$ (402·3): calculated C 47·77 per cent, H 2·51 per cent, N 13·93 per cent; found C 47·82 per cent, H 2·50 per cent, N 13·85 per cent.

2.1.2. *2-(6-Hydroxyhexyloxy)-3,6,7,10,11-pentakis(pentyloxy)-triphenylene* 7

Compound 7 was synthesized by a method analogous to that described earlier by Kreuder [22]. The following modifications were made. 2 g (2·8 mmol) of 3,6,7,10,11-pentakis(pentyloxy)-2-triphenylenyl acetate 6 [9,23,24], 1·8 g (12·8 mmol) of dried powdered K$_2$CO$_3$, 0·5 g (3 mmol) of KI and 2·3 g (12·8 mmol) of 6-bromohexanol in 40 ml of dry ethylmethylketone were refluxed for four days under an argon atmosphere. The reaction mixture was then filtered and the residue was extracted several times with CH$_2$Cl$_2$. The combined organic solutions were washed with 1N H$_2$SO$_4$, several times with water and dried over Na$_2$SO$_4$. After evaporation of the solvents and the remaining bromohexanol the crude product was purified twice by flash chromatography with CH$_2$Cl$_2$/methanol (volume ratio 300 : 1) as eluent. The procedure yielded 1·5 g (69 per cent) of a slightly brownish solid which was taken for further reaction. Purification was only performed after the final step.

2.1.3. *3,6,7,10,11-Pentakis(pentyloxy)-2-triphenylenyl-β-(2,4,7-trinitro-9-fluorenylideneaminooxy)propionate* **1**

2 g (2·8 mmol) of **6**, 1·4 g (3·5 mmol) of **5** and 3 mg ($1·6 \times 10^{-2}$ mmol) of 4-toluenesulfonic acid monohydrate were melted in a 10 ml flask. The temperature was successively decreased from 210°C down to 160°C during the first hour. The acetic acid formed was removed under reduced pressure ($p < 10^{-3}$ mbar). After nine hours the reaction was finished. The product was then isolated by twofold flash chromatography with CH_2Cl_2/petroleum ether as eluent (volume ratios: (*a*) 3 : 2, (*b*) 2 : 1). The product was dissolved in pure CH_2Cl_2, filtered and then pure ethanol was added until solid particles appeared. After heating the mixture, cooling at -20°C overnight and separation by means of a centrifuge resulted in 1 g (34 per cent) of a reddish solid.

IR (KBr): $\tilde{v} = 1764$ cm^{-1} (C=O). ^{1}H NMR (400 MHz, CDCl$_3$): δ (ppm) = 8·20–6·10 (m; 11 H, arom. H), 4·58 (s; 2 H, N–O–CH$_2$), 4·10–3·73 (m; 6 H, 3 × O–CH$_2$), 3·61 (s; 2 H, O–CH$_2$), 3·36 (s; 2 H, O–CH$_2$), 3·25 (s; 2 H, O–CO–CH$_2$), 1·88 (s; 6 H, O–CH$_2$–CH$_2$), 1·68 (s; 2 H, O–CH$_2$–CH$_2$), 1·52–1·10 (m; 22 H, CH$_2$), 1·02 (m; 15 H, 5 × CH$_3$). All signals are very broad. Those of the α-methylene groups of the pentyloxy side chains are split in the ratio 6 : 2 : 2 without the possibility of exact differentiation of the positions. MS (FD): *m/e* (per cent) = 1059 (MH$^+$, 100). UV-Vis(CH$_2$Cl$_2$): λ_{max}/nm (log ε) = 277 (5·0). C$_{59}$H$_{70}$N$_4$O$_{14}$ (1059·2): calculated C 66·90 per cent, H 6·66 per cent, N 5·29 per cent, found C 67·01 per cent, H 6·45 per cent, N 5·25 per cent.

2.1.4 *6-[3,6,7,10,11-Pentakis(pentyloxy)-2-triphenylenyloxy]-hexyl-β-(2,4,7-trinitro-9-fluorenylideneaminooxy) propionate* **2**

The procedure followed a modification of the DCC method. 1·5 g (1·9 mmol) of **7** and 2·5 g (6·5 mmol) of **5** were dissolved in 8 ml of dioxane p.a. by heating. After the addition of 5 ml of CH$_2$Cl$_2$ p.a. the reaction vessel was sealed under nitrogen atmosphere with a septum and cooled to 0°C. Thereafter a trace of DMAP in 0·5 ml of CH$_2$Cl$_2$ p.a. and over a period of 30 min 1·35 g (6·5 mmol) of DCC in 1·5 ml of CH$_2$Cl$_2$ p.a. were injected using a syringe. The reaction mixture was allowed to warm overnight and stirred at room temperature for five additional days. After evaporating the solvents the product **2** was separated from most of the by-products in an initial flash chromatography step with toluene as solvent (eluation volume approximately 20 l). The threefold recrystallization with methanol/CH$_2$Cl$_2$ (volume ratio 1 : 1) resulted in 1 g of raw material. Hereupon the product was purified by a second flash chromatography with CH$_2$Cl$_2$/petroleum ether (volume ratio 3 : 2) as eluent. Mixed fractions were treated once more in the same manner. Finally the collected products were recrystallized as described for compound **1**. Yield: 730 mg (33 per cent) of a dark red solid.

IR (KBr): $\tilde{v} = 1736$ cm^{-1} (C=O). ^{1}H NMR (400 MHz, CDCl$_3$): δ (ppm) = 8·53 and 8·50 (2d, $J_{3-1} \sim 2$ Hz; 1 H, TNF-H^3), 8·28 and 8·16 (2d, $J_{1-3} \sim 2$ Hz; 1 H, TNF-H^1), 7·99, 7·97 and 7·95 (3d, $J_{6-8} \sim 2$ Hz, $J_{6-5} \sim 8$ Hz; 1 H, TNF-H^6), 7·90, 7·83 and 7·80 (3d, $J_{8-6} \sim 2$ Hz; 1 H, TNF-H^8), 7·64 and 7·62 (2s, $J_{5-6} \sim 8$ Hz; 1 H, TNF-H^5), 7·43–7·33 (m; 6 H, arom. H of triphenylene), 4·65 (m; 2 H, N–O–CH$_2$), 4·30 (m; 2 H, CO–O–CH$_2$), 4·08 (m; 12 H, O–CH$_2$), 2·88 (m; 2 H, O–CO–CH$_2$), 1·93 (m; 12 H, O–CH$_2$–CH$_2$), 1·81 (m; 2 H, CO–O–CH$_2$–CH$_2$), 1·68–1·43 (m; 24 H, CH$_2$), 0·98 (m; 15 H, CH$_3$). MS (FD): *m/e* (per cent) = 1160 (MH$^+$, 100) 830 (50). UV-Vis(CH$_2$Cl$_2$): λ_{max}/nm (log ε) = 278 (5·0). C$_{65}$H$_{82}$N$_4$O$_{15}$ (1159·4): calculated C 67·34 per cent, H 7·13 per cent, N 4·83 per cent; found C 67·21 per cent, H 7·04 per cent, N 4·75 per cent.

2.2. *Characterization of the samples*

Absorption spectra were recorded on a Perkin–Elmer spectrometer with a concentration of 5×10^{-6} mol 1^{-1}. With higher concentrations of compounds **1** and **2** (10^{-4} to 10^{-3} mol 1^{-1}) a broad charge-transfer band appears (400–700 nm).

The optical textures were analysed with a Leitz Orthoplan polarizing microscope equipped with a Mettler FP 82 hot stage. Calorimetric investigations were performed using a Perkin–Elmer DSC-4. The heating and cooling rates amounted to 20 K min^{-1}. Results are only presented which were obtained in the second heating run.

Oriented samples were obtained for the X-ray analysis in two different ways: by employing a simple shearing procedure in the liquid-crystalline state near the clearing temperature, and by applying a planar pressure in a cell allowing only a unidirectional flow in one direction perpendicular to the direction of pressure [25].

X-ray diagrams for oriented systems were recorded on a flat plate camera. WAXS curves were obtained with a Siemens D-500 diffractometer using step-by-step scanning. The scanning steps amounted to 0.05–$0.1°$. SAXS curves were obtained employing a compact Kratky camera equipped with a position sensitive detector. Ni filtered CuK$_\alpha$-radiation was used in all cases. All samples studied were melted and annealed prior to subjecting them to the X-ray analysis. The program FIT was used for the analysis of the shape of the scattering profiles and for separating overlapping peaks. The program includes the subtraction of the background, smoothing by splines and a fit of the profiles to various scattering functions (lorentzian, gaussian etc.) [26]. To model the packing of the molecules and to assign the interatomic distances obtained from scattering studies computer models were constructed by means of the Biosym program INSIGHT and the most favourable conformation of the molecules was calculated by using the program DISCOVER (Biosym) on a Silicon Graphics workstation [27].

3. Experimental results and discussion

3.1. *The structural ordering in compound* **1**

It is apparent from optical microscopic and calorimetric studies that an enantiotropic mesophase exists for **1** over a broad temperature range extending up to 265°C. A bright but unspecific optical texture was observed in this temperature range. The DSC curves indicate two transitions during a first and second scan. The corresponding data for the second scan are collected in table 1. The first of them corresponds to a glass transition and the second one to the clearing temperature as observed by polarization microscopy. No decomposition for either compounds was detected by DSC but slight changes of colour were observed after prolonged periods near the clearing temperature.

Table 1. Transition temperatures and clearing enthalpies of **1** and **2** as determined by DSC.

Compound	$T_g/°C$†	$T_i/°C$‡	$\Delta H/\text{kJ mol}^{-1}$§
1	50	265 dec.‖	10·6
2	14	242 dec.‖	11·9

† Glass transition temperature.
‡ Clearing temperature.
§ Clearing enthalpy.
‖ Observed under the microscope during annealing the compound near the clearing temperature.

The high clearing temperature and the very broad temperature range in which the liquid-crystalline phase is stable are unusual features particularly in view of the low-molecular weight nature of the system considered here. Corresponding 1 : 1 mixtures of low molecular weight donors and acceptors of the same nature, as a rule, show mesophases only for lower temperatures and furthermore these systems tend to crystallize [15, 25]. Cooling the systems **1** and **2** to room temperature leads to the formation of an optically anisotropic glassy state.

The X-ray scattering curves obtained for remelted and annealed samples reveal the existence of a surprisingly large number of sharp peaks in the small-angle range: it is possible to distinguish at least four peaks for **1** with strong differences in their intensity and overlapping of the second and third peak (resolution of these maxima was performed by fitting to lorentzian profiles) (see figure 2 (a)). Furthermore we detect a sharp peak overlapped with a diffuse halo in the wide-angle range (see figure 2 (b)). The periodicities for all observed peaks calculated from the positions of the corresponding fits to lorentzian profiles (R-factors are 2–4 per cent) on the basis of Bragg's law are presented in table 2.

For oriented samples 'two-point' diagrams were obtained. For sheared **1** the reflection ($1\bar{1}0$) (the assignment of the reflections will be discussed later) makes an azimuthal angle of 30–40°, the other two reflections (100) and (200) are strongly broadened (see figure 3 (a)). For samples oriented by pressure we find that the reflections ($1\bar{1}0$) in the small angle region are slightly tilted with respect to the equatorial plane (see figure 3 (b)). The other sharp reflections (100) and (200) are strongly broadened in the azimuthal direction and centred about an azimuthal angle of 50–60°. In both cases the wide-angle X-ray scattering is located in very diffuse arcs. This, and the high azimuthal spreading of all reflections, evidently originates from a poor macroscopic orientation of both samples.

Table 2. Bragg reflections and indexation of cells of **1** and **2**.

		Distances						
		SAXS†				WAXS‡		
ompound		d^1/nm	d^2/nm	d^3/nm	d^4/nm	D^1/nm	D^2/nm	D^3/r
	Distance (meas.)	2·5	1·9±0·05	1·56	1·22	0·68	0·43	0·3
1	Index§ (orthorhomb.)	100	010	$1\bar{1}0$	200	001	—	00?
	Distance (calc.)	2·5	1·85–1·95	1·48–1·55	1·25	0·68	—	0·3
	Distance (meas.)	—	1·52	1·35	—	0·68	0·44	0·3
2	Index§ (orthorhomb.)	—	010	110	—	101	—	20?
	Index§ (hex.)	—	100	110	—	001	—	00?

† d^i-Bragg distances for SAXS peaks; accuracy = 0·02 nm.
‡ Bragg distances for WAXS peaks (D^1, D^3) and diffuse halo (D^2); accuracy = 0·002 nm.
§ Miller indexes for various peaks and corresponding calculation of the distances (d^i and D^i) :horhombic (**1** and **2**) and hexagonal cell (only **2**).
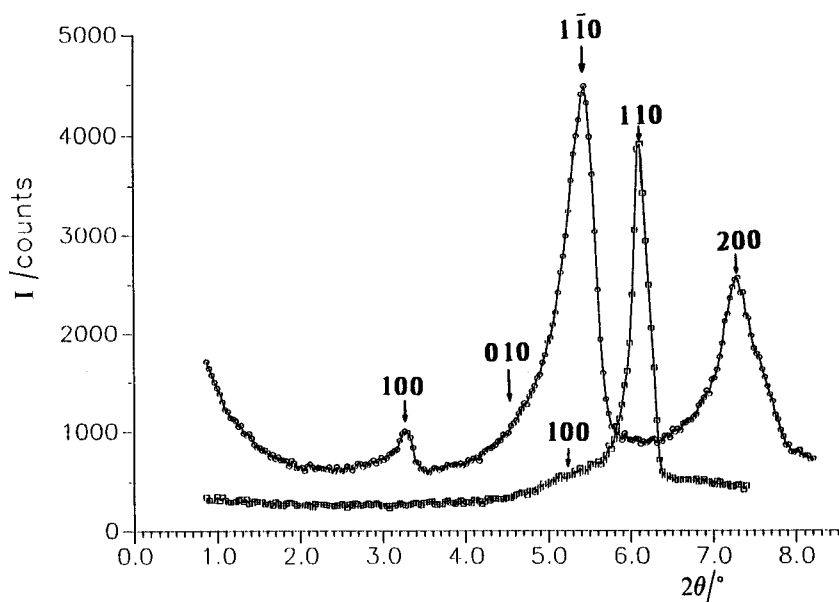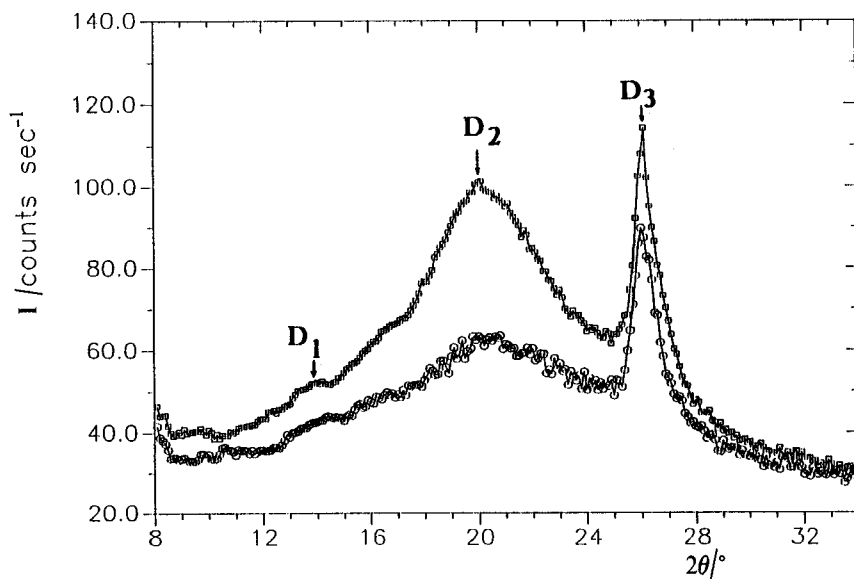
Figure 2. X-ray scattering data for **1** (○) and **2** (□) (room temperature, powder samples): (*a*) small-angle curves; (*b*) wide-angle curves. Markers of the peaks correspond to those in tables 2 and 3.

M. Möller *et al.*

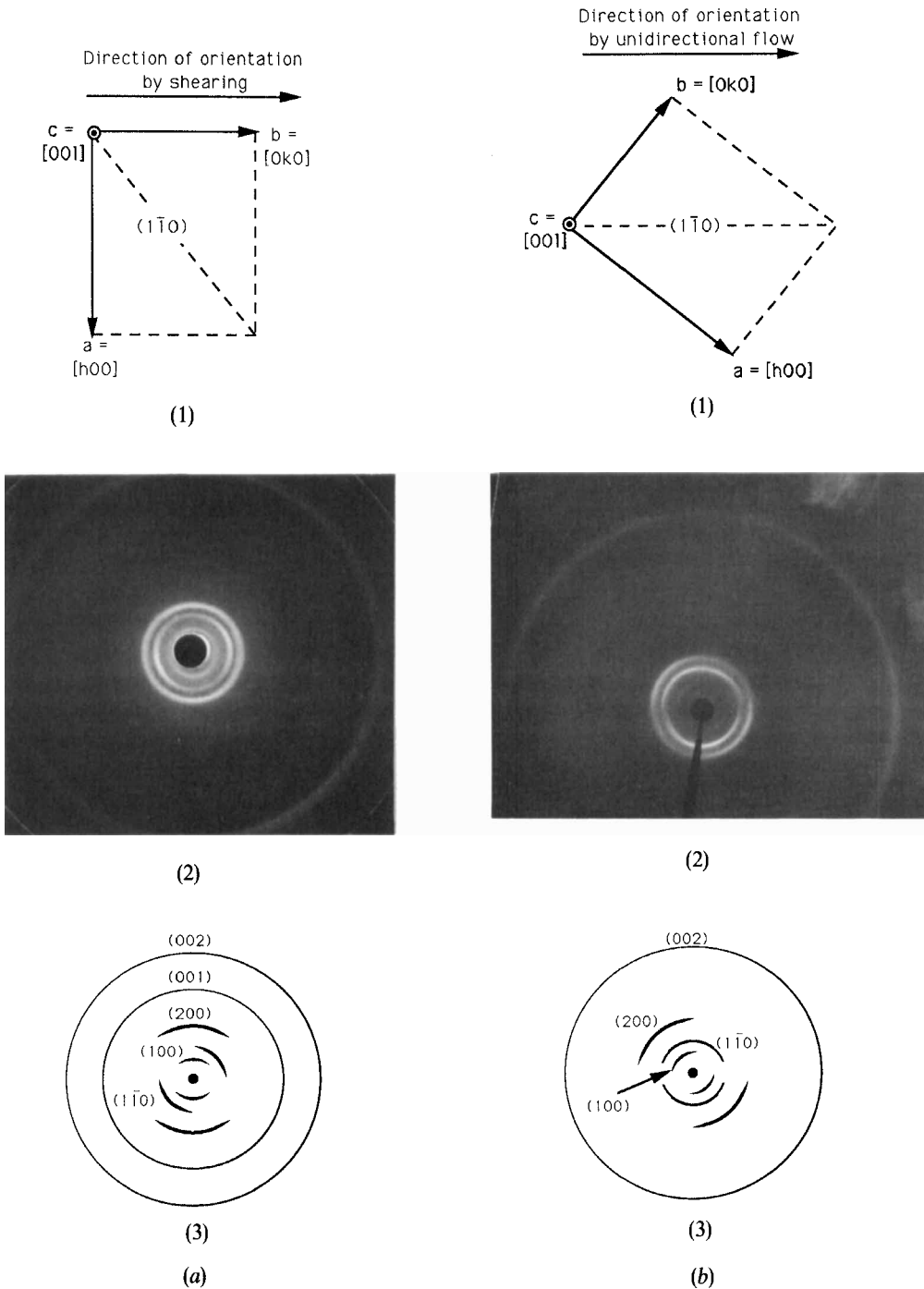Figure 3. Structural data for sample **1** oriented by (*a*) shearing and (*b*) undirectional flow: 1. the schemes of orientations of unit cell edges; 2. X-ray patterns for oriented samples (the weak wide-angle maxima are not visible); 3. the corresponding schematic X-ray diagrams.

3.1.1. *Intracolumnar ordering*

The wide angle pattern obtained for compound **1** is characteristic for discotic systems forming columns. A similar pattern has been observed for mixtures of triphenylene and TNF derivatives [25(a)]. The sharp peak on the WAXS curves ($d = 0.34$ nm) is thus attributed to the 002 order of reflection for dense plane-by-plane packing of the rigid aromatic cores in columns and the diffuse halo to the more disordered packing of the side chains and spacers [25(a), 28]. An additional weak peak with a periodicity of 0·68 nm is also detected on the WAXS curves and X-ray patterns (see figures 2(b) and 3). It corresponds, as was shown in [15, 25(a)], to the formation of mixed intracolumnar stacks with alternating packing of the different cores. Such an alternating intracolumnar packing gives rise to a density distribution wave along the axes of columns with a main period of 0·68 nm (the distance between the triphenylene cores). An additional half-period density wave should be formed by the incorporated TNF molecules [25(a)]. In such cases the odd orders of reflections (001, 003, . . .) should be weaker than the even ones as was shown earlier for such density distributions by a direct calculation of the structure factor [25(b, c)]. Thus the experimentally observed ratio between the intensities for the 001 and 002 orders of reflection points strongly to the formation of an alternating intracolumnar packing and not a random mixed one.

3.1.2. *Intercolumnar ordering*

For mixtures of triphenylenes and TNF derivatives columnar mesophases have been observed with a hexagonal ordering of the columns [17, 25(a), 29]. As a rule only two orders of reflections having Miller indexes (110) and (100) (sometimes (200)) were observed at positions appropriate for such hexagonally ordered columnar structures [25(a), 29]. The small-angle curve characteristic of **1** displays, however, a large number of sharp reflections and a complex modulation of their intensities with the order of the reflections. These features reflect obviously the existence of an intercolumnar packing of a non-hexagonal type. Based on model calculations for some trial lattices we have chosen an orthorhombic cell with parameters a, b, c given in table 3 as a satisfactory representation of the packing of the columns. The calculated positions of various orders of reflection correlate very well with those observed (see table 2).

It is possible to pack molecules of **1** in various manners in this cell. Comparison of the geometric sizes of the molecules and the cell parameters suggest a diagonal arrangement of the molecules in the $a \times b$ plane (see figure 4(a)). Two repeat units are packed in the unit cell, the location of the second unit being around the centre. Such an arrangement of repeat units is very similar to that known for the non-primitive, orthorhombic body centred cell [28, 30]. For an ideally body-centred cell all odd

Table 3. Parameters for the cells and corresponding thermal expansion coefficients of **1** and **2**.

	Lattice	a/nm	b/nm	c/nm	$K_a/10^4\,°C^{-1}$	$K_b/10^4\,°C^{-1}$	$K_c/10^4\,°C^{-1}$
1	Orthorhombic	2·5	1·95	0·68	1·7	3·5	1·7
2	Orthorhombic	2·9	1·52	0·68	2·5‡	3·5	1·7
	Hexagonal	1·52	—	0·68	—	—	—

† For **2** two possible parameters of the cells are calculated for two different sets of indexes (see table 2).

‡ K_a corresponds to the normal to the (110) plane.
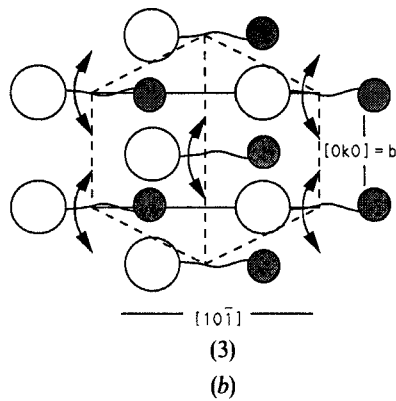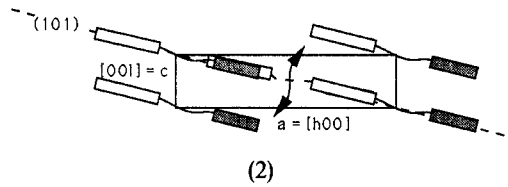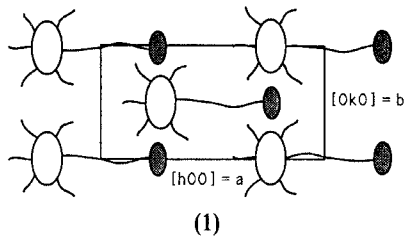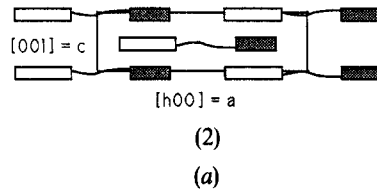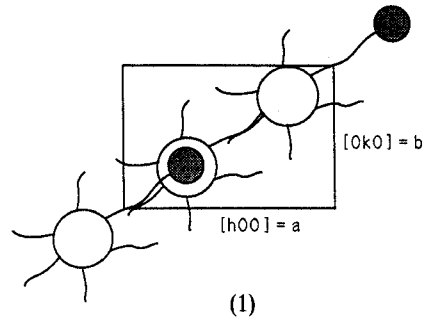
Figure 4.   Proposed models for the arrangement of the disc-like repeat units in an orthorhombic
cell for **1** (*a*) and **2** (*b*): 1. along the normal to the *a* × *b* plane; 2. along the normal to the *a* × *c*
plane; 3. along the normal to the (101) plane (only for **2**); the arrow in figure 4 (*b*) part 2
refers to the body centred molecule (see text). All molecules are presented by the sketches to
avoid complexity; real molecular sizes can be obtained from figure 8.

reflections with $(h00), (0k0), (00l) = 2n + 1$ should be absent. We observe, however, weak traces of $(h00), (0k0), (00l)$ orders of reflections (see figures 2(a) and (b)). Our interpretation is, that the molecules within the liquid-crystalline state are not located exactly at the centre but are shifted by about 0·1–0·3 nm away from it, in contrast to the ideal crystalline state. This would give rise to the weak traces of the forbidden reflections. It seems that such shifts are a characteristic feature of the liquid-crystalline state as compared to the crystalline state.

The proposed cell allows us to explain other characteristic features observed experimentally.

(i) First, consider the macroscopic density. The corresponding calculations of the density based on the proposed parameters of the cell and on the known molecular weight lead to a value of about 1·1 g cm^{-3}, which corresponds quite well to the measured value (1·12 g cm^{-3}).

(ii) Secondly, the observed data for samples oriented by unidirectional flow are consistent with columns arranged orthogonally to the direction of orientation (see figure 3). The planes of the aromatic cores ($a \times b$ plane which corresponds to Miller indexes $(hk0)$) become oriented parallel to the external stress (see figure 5(a)). For such a model the corresponding reflections (100) and (200) should be arranged at an angle of $\varphi = 38°$ with respect to the meridional plane. This corresponds very well to the experimentally observed azimuthal location (see figure 3(b)). A similar situation is observed for sheared samples. The (001) and (002) reflections are arranged normal to the observation plane and we are able to see only weak traces of the intersection of the observation plane and the azimuthally broadened (00l) reflections (see figure 3(a)).

(iii) The third point to consider is the thermal expansion behaviour. The increase of the lattice parameters representing the intercolumnar and intracolumnar packing with temperature is practically linear for the whole temperature range and for all reflections (see figure 6). The absolute values for the corresponding thermal coefficients K_i along the a, b and c directions of the lattice calculated from the relationship

$$K_i = (d^i(T^i) - d^i(T^0))/((T^i - T^0)d(T^0))$$

are in the range of 10^{-4} °C^{-1} (see table 3) which is typical for liquid-crystalline polymers [25, 31]. The thermal expansion controlled by the intercolumnar ordering in the $a \times b$ plane is, however, strongly anisotropic: the thermal expansion along the a axis is much lower than along the b direction. These features will be discussed later in more detail.

3.2. *The structural ordering in compound* 2

The DSC data for compound 2 correspond closely to those reported for 1. They indicate the presence of a glass transition temperature (see table 1) at low temperatures and a melting endotherm is observed at a temperature of about 240°C. Polarizing microscopic investigations show that a liquid-crystalline state is stable up to this temperature where a transition into the isotropic melt takes place. The texture shows a typical fractal type pattern which is frequently observed for hexagonally packed discotic phases [32].

The X-ray pattern obtained for 2 contains fewer reflections than those of compound 1. Only two are found in the small-angle region (see figure 2(a)), whereas the wide-angle

Direction of orientation
by unidirectional flow

[h00] = a

[0k0] = b

Direction of
orientation
by shearing

(a)

Direction of orientation
by shearing

[001] = c   a = [h00]

(b)

Direction of orientation
by unidirectional flow
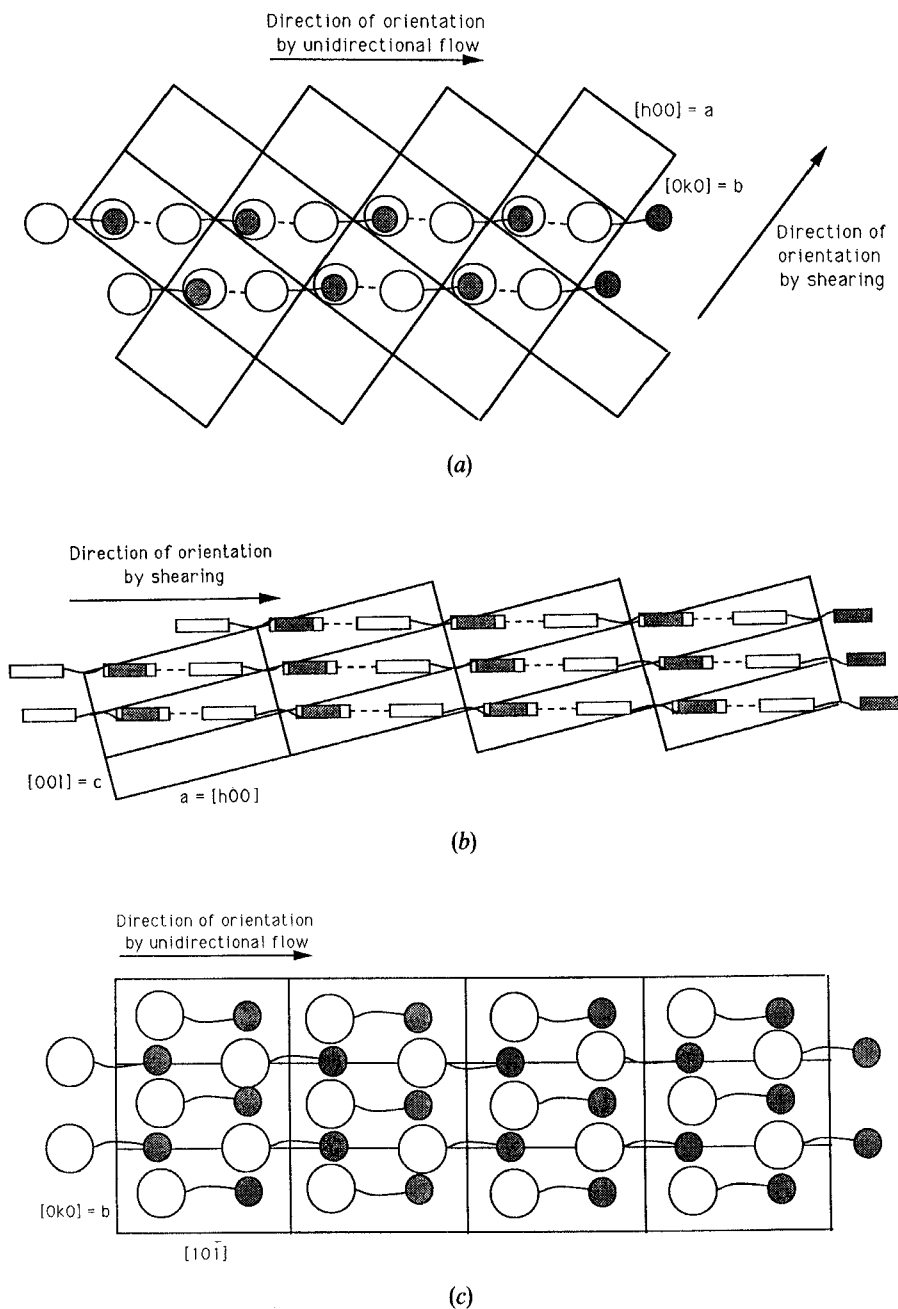
[0k0] = b

[10$\bar{1}$]

(c)

Figure 5.   Orientation of the lattice planes according to the orientation direction for 1 (*a*) and for
2 (*b*) shearing, (*c*) unidirectional flow (without indicating the mobility, see also figure 4 (*b*) 2)
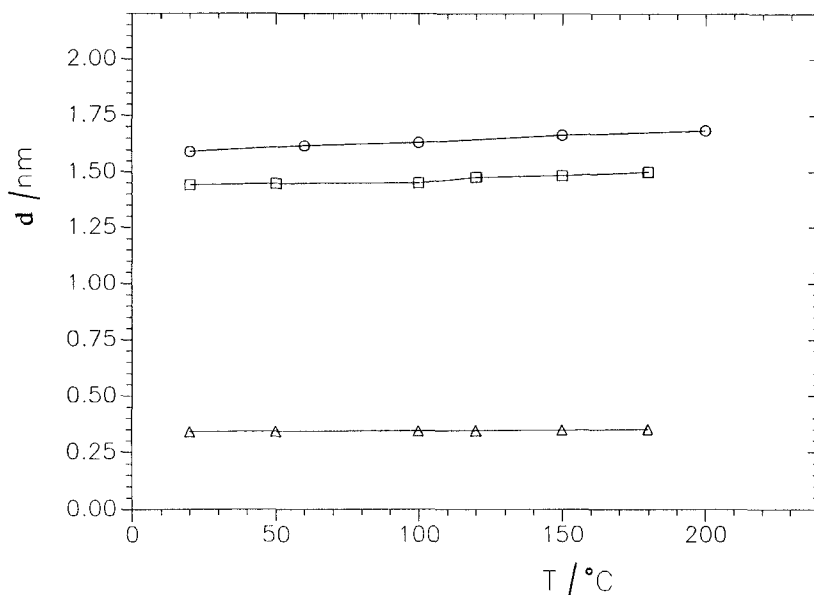and the corresponding schemes for the molecular arrangement.

Figure 6. Example of the temperature dependence of the various d spacings for: 1 (1$\bar{1}$0), 3 (002) for **1**; 2 (110), 3 (002) for **2**. ($\bigcirc$) 1, ($\square$) 2, ($\triangle$) 3.

scattering is identical to that described for **1** (see figure 2(b)). The last point has to be taken as an indication of the presence of an alternating columnar structure. The presence of only two small-angle peaks makes a detailed analysis of the symmetry and of the cell parameters very difficult: it is possible to propose various cells and types of arrangements of molecules.

Samples oriented by shearing display small-angle peaks which are arranged on the meridional plane (according to the direction of orientation) while in the wide-angle range a spread azimuthal distribution is observed for the diffuse halo and the narrow reflections (Bragg analysis: 0·68 and 0·34 nm), (see figure 7(a)). From the equatorial position of the sharp WAXS maximum and the meridional position of the SAXS reflection we can conclude immediately that the columns are oriented normal to the direction of orientation. For this system the planes of the rigid cores are oriented along the direction of orientation and the b edges of the cells are arranged normally to the direction of orientation (see figure 5(b)). Thus the overall orientation of the lattice in oriented **2** is different to that in **1**.

Another type of X-ray pattern was obtained for samples oriented by unidirectional flow (see figure 7(b)). In this case a clear six point diagram is observed, the only periodicity being about 1·5 nm. No additional reflections are visible for such a type of orientation. This pattern seems to indicate the presence of a hexagonal ordering of the columns. It can, however, also be explained within the framework of the model proposed for **1**. The observed behaviour is easy to understand if we assume that the planes of the discs in the repeat units are located around the ($h0l$) planes (see figure 4(b)). For such an arrangement the cell can be classified as orthorhombic with a tilted arrangement of the disc planes or as a common hexagonal cell with normal arrangement of the discs in the (101) plane (see figures 4(b) and 5(b)-(c)). The exact
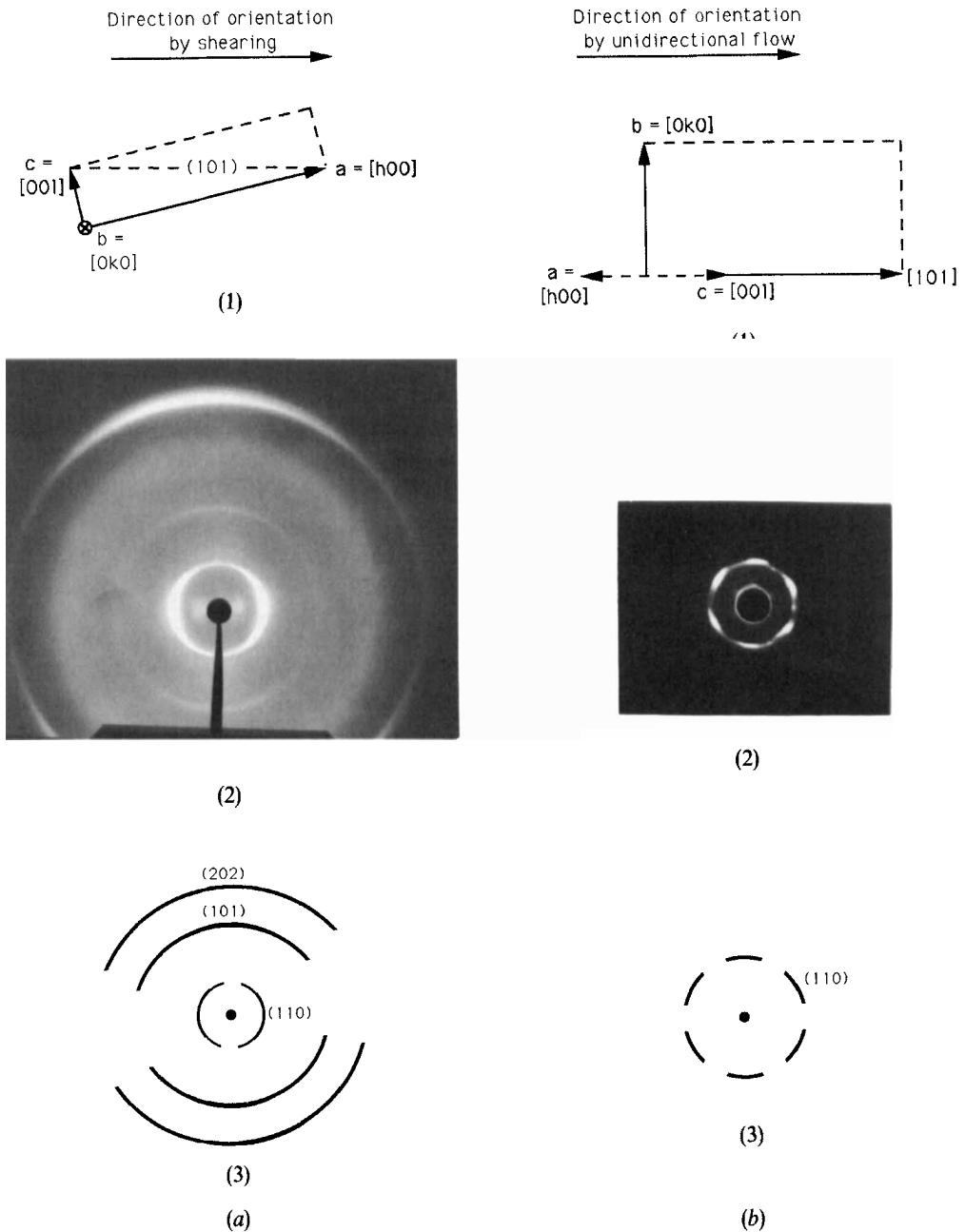
Figure 7.   Structural data for sample **2** oriented by shearing (*a*) and unidirectional flow (*b*): 1, the schemes of orientations of unit cell edges; 2, X-ray patterns for oriented samples (scattering near the beam stop is the trace of a primary beam); 3. the corresponding schematic X-ray diagrams; (for figure 8 (*b*) 1 the *a*- and *c*-edges are arranged out of the plane of the figure).

orientation of the molecules in this plane may not be well deduced from the present X-ray data. Preliminary deuterium NMR measurements of **1** and **2** deuteriated in the triphenylene core positions actually show that the acceptor is quite mobile in the liquid-crystalline phase of **2**. As a result the exact position of the acceptor unit in the mesophase cannot be determined. This is contrary to **1** where a similar process could not be observed [33].

The different X-ray patterns observed for **2** oriented either by shearing or unidirectional flow originate thus from different arrangements of the columns with respect to the direction of orientation: for the sheared sample the $a \times b$ planes of the cells are oriented along the direction of orientation and columns lie orthogonal to the direction of orientation and primary beam. In the sample oriented by unidirectional flow the planes of the molecules are arranged parallel to the direction of flow and thus the columns are arranged along the direction of the primary beam (see figure 7).

The analysis of the structural data leads thus to two most probable descriptions for the molecular packing for sample **2**: the same orthorhombic cell as proposed for **1** with another set of cell parameters and a specific arrangement of the molecules in the repeat unit, or a common columnar structure with a hexagonal symmetry (see figures 4 (*b*) and 5 (*b*)–(*c*)). The final selection of the most probable model can only be made on the basis of the analysis of additional data and direct calculations of the structure factors.

Some additional features characteristic of **2** will briefly be considered next. Calculations of the density based on the proposed parameters of the cell and the molecular weight lead to the value of density ($1.05\,\mathrm{g\,cm^{-3}}$) which corresponds quite well to that measured of $1.07\,\mathrm{g\,cm^{-3}}$ for **2**. In addition the thermal expansion of the intercolumnar ordering in the $a \times b$ plane is again very anisotropic (see table 3).

In the following, differences and similarities of the proposed models for both compounds are discussed.

3.3. *Features of the molecular packing of* **1** *and* **2** *formation of mixed stacks*

As judged from the analysis of WAXS data both systems have the same type of local intracolumnar packing of the molecules in the c direction with an alternating sequence of donors and acceptors (see figure 4). Evidently, besides charge transfer interactions, an additional driving force for the formation of such alternating stacks is the great volume difference of the triphenylene and TNF parts of the molecules.

### 3.3.1. *Orientations of the repeat units in the cell*

From the corresponding conformational calculations some additional conclusions can be drawn on the mutual arrangement of the donor and acceptor moieties. These calculations suggest that the planes of the triphenylene and TNF discs lie almost parallel (see figure 8). This allows the formation of a perfect intracolumnar packing with periodicities close to the minimal possible distances between two plane-by-plane packed phenyl rings. With respect to the arrangement of the flexible tails of the triphenylene disc, it is evident that variations of the torsional angles at the location of their attachments to the rigid disc leads only to slight changes of the conformational energy. Thus in densely packed systems these flexible tails can be arranged in various ways (as in amorphous systems) to fill the space available to them in the cell.

3.3.2. *Conformation of the flexible spacers*

No direct information is available on the conformation of the flexible spacers. Computer simulations using the programs INSIGHT and DISCOVER show that the conformation of the cores is rigid while the variations of the torsional angles of the

M. Möller *et al.*

(*a*)
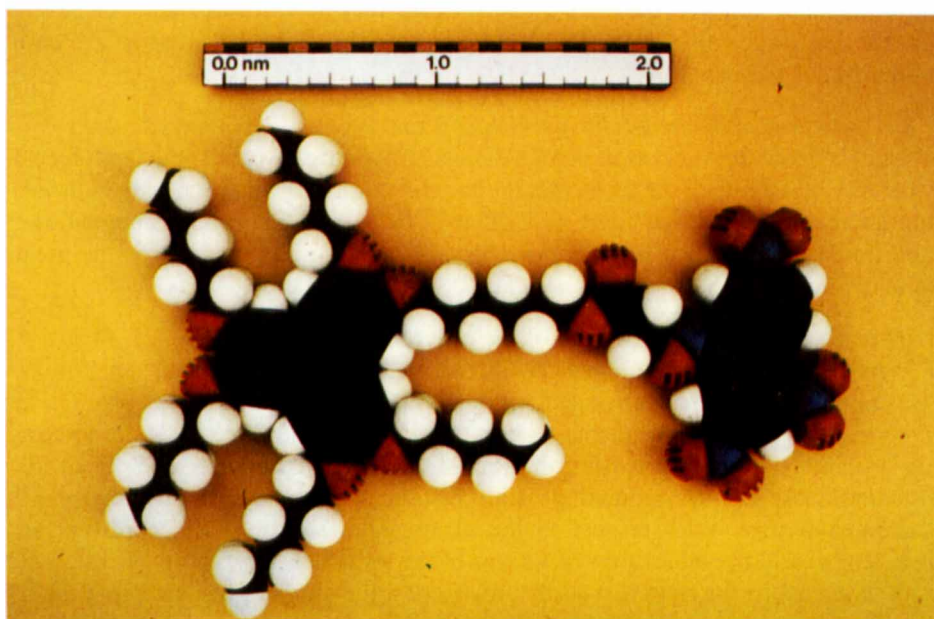
(*b*)

Figure 8.   Space filling models of the molecules: **1** (*a*) and **2** (*b*).

flexible tails and spacer lead only to minor changes in the overall energy of the molecules. From this point of view the probabilities of the extended or disordered (with the presence of some *gauche* conformers) conformations for tails and spacers are very close. As deduced from these calculations the occurrence of small deviations from the fully extended conformation could lead to a parallel arrangement of the triphenylenes and TNF fragments in different planes which is sketched in figure 4(b) (see arrows).

3.3.3. *Perfection of order: spatial correlations in intra- and intercolumnar packing*

(a) *Intracolumnar correlations*

To obtain more detailed information on the order of the intracolumnar packing we have analysed the WAXS scattering peaks (sharp reflection and halo) separately. The decomposition of the overlappings peaks was performed by fits to various scattering functions. The best fit was obtained for lorentzian profiles which corresponds to an exponential damping of the correlations. This is typical for liquid-crystalline polymers [31]. From the lorentzian profiles the corresponding correlation lengths ξ were calculated (the sizes of ordered regions L are connected with the values of ξ by $L = 3\xi$ [31]). As apparent from table 4 the values of ξ^s for intracolumnar correlation are approximately the same for both samples (about 3 nm) and correspond to a high level of ordering extending over 30–40 neighbouring molecules. The level of short range ordering of the flexible fragments is typical for amorphous systems: the values of ξ^d are in the same range for both compounds and slightly higher in **2** than in **1** (see table 4).

(b) *Intercolumnar correlations*

From the analysis of the shapes of the SAXS reflections conclusions about the extent of the intercolumnar ordering can be drawn. All small-angle peaks could be fitted well to lorentzian functions, the absolute scales of the correlation lengths for different orders of reflections were, however, different (see table 4). For **1** the value of ξ^i for the most intense ($1\bar{1}0$) peak is equal to 19 nm, for the (100) peak it is 12 nm, and for the (010) peak it amounts to only 5 nm. The strongest correlations exist in the direction normal to the diagonal (110) plane and along the *a* axis of the orthorhombic lattice. Only very weak translational correlations are observed along the *b* axis of the lattice. Thus a rather perfect quasi-long range ordering with a correlation of the order of some tens of columns is realized for the packing of columns along the normal to the (110) and (100) planes. A similar situation is observed for **2**: strong correlations exist only along the (110) plane (see table 4).

Table 4. Correlation lengths for **1** and **2**.

	Correlation lengths†‡				
	ξ^d/nm	ξ^s/nm	ξ^1/nm	ξ^2/nm	ξ^3/nm
1	0·3	3	12	19	5
2	0·4	3·1	2·8	23	——

† ξ^d, ξ^s-correlation lengths in intracolumnar packing calculated from lorentzian profiles for a diffuse halo and a sharp peak.

‡ ξ^i-correlation length for *i*-SAXS peak calculated from lorentz profiles: ξ^1, ξ^2 and ξ^3 correspond to **1** with directions [100], [110] and [010] and for **2** (hexagonal indexation) [100] and [110], respectively.

Such a one dimensional ordering of the intercolumnar packing is a special feature of the systems studied here as compared to common columnar mesophases. As a result of the covalent linkage of donor and acceptor, each column is connected in one direction with two neighbouring columns chemically via flexible spacers: along the diagonal of the $a \times b$ plane of the lattice in compound **1**, and along the diagonal of the $a \times c$ plane for compound **2** (see figures 4 and 5). Taking into account the fact that the molecules in the columns are connected with others through charge transfer interactions (see §2), a one dimensional quasi-macrochain propagates along into the named directions for some tens of neighbouring unit cells. Only weak van der Waals interactions exist, on the other hand, along the direction perpendicular to this macrochain. Such a situation should lead to a strong anisotropy of the spatial ordering along the different directions in the lattice (see figures 4 and 5, and table 4).

Starting from the proposed concept of the existence of one dimensional quasi-chains it is also possible to explain the observed anisotropy of the thermal expansion and the orientational behaviour. As known from the data for common polymers the chain backbone is frequently oriented along the direction of flow (external field). Therefore it is plausible that in oriented samples the $a \times b$ planes of **1** and the (101) planes of **2**, contain the planes of discs, are aligned parallel to the flow. A direct analogy leads to the conclusion that the overall orientation of the lattice is determined by the elongation of the quasi-chain along the orientation direction.

4. General discussion and conclusions

The linking of disc-like donor and acceptor molecules via flexible spacers of various lengths leads to the formation of a very stable mesophase with glass transitions near room temperature and a broad phase width with clearing temperatures around 240–260°C.

Both systems form specific types of mesomorphic order with features of different classes of liquid crystals. On the one hand they possess a columnar type of molecular packing typical for discotic systems. On the other hand they display only a one dimensional long range ordering with respect to the intercolumnar packing which is typical for smectic phases. They might be described as exhibiting an orthorhombic columnar phase with $a \neq b$ (**1**) or as displaying an orthorhombic columnar phase with tilted planes of the discs or as a hexagonal phase (**2**) (see figures 4 and 5). Therefore compounds **1** and **2** can be considered as intermediates between classic columnar discotic phases and smectic phases (see figure 9). Such an idea was already discussed earlier but for another class of compounds [14].

The chemical link of donor and acceptor leads to the formation of an alternating stacking of the molecules along the c direction. Long range correlations in the plane-by-plane packing of the discs are observed with an expansion of the correlations to 30–40 neighbouring rigid cores. Despite the high level of perfection in the intra-columnar packing of rigid disc-like cores the long flexible spacers and tails are in a disordered, amorphous state.

As a result of both, the formation of alternating stacks of donor and acceptor moieties and the flexible spacer (covalent link) along the diagonal of the $a \times b$ plane in compound **1**, and along the diagonal of the $a \times c$ plane for compound **2**, a very peculiar one dimensional quasi-chain is realized. The neighbouring columns are connected via such quasi-chains in one special direction for each compound. Such differences in the
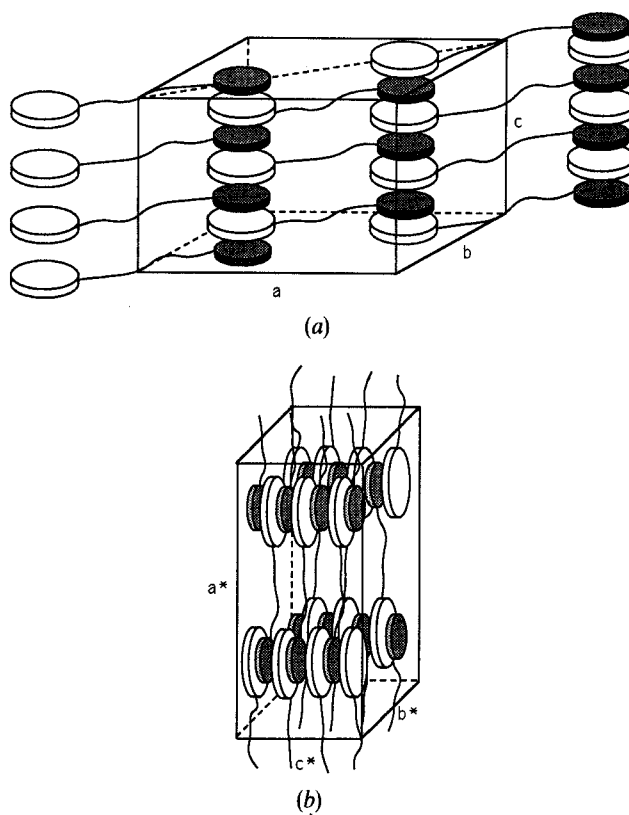
(a)

(b)

Figure 9. Possible approaches for the description of molecular ordering in the systems studied: (a) columnar phase with orthorhombic lattice; (b) orthogonal smectic-like structure with one dimensional ordered intralayered packing.

nature of the intercolumnar contacts of the columns in various directions are responsible for a number of specific features of such systems:

(i) formation of orthorhombic symmetry of intercolumnar packing instead of common hexagonal;

(ii) different distribution of the spatial correlations in the intercolumnar packing in various directions: in the directions of connection of columns via quasi-chains a long range translational ordering is realized while in the opposite directions only short range ordering of a liquid-like type is realized;

(iii) the overall orientation of the lattice is determined by the orientation of the quasi-chain along the direction of orientation;

(iv) an anistropy in the thermal expansion along the different directions of the lattice is determined by the arrangement of the quasi-chains: along these directions, thermal expansion is much lower than in the orthogonal directions.

References

[1] BRYCE, R., and MURPHY, L. C., 1984, *Nature, Lond.*, **309**, 119.

[2] WEGNER, G., 1981, *Angew. Chem.*, **93**, 352; 1981, *Angew. Chem. Int. Ed. Engl.*, **20**, 361.

[3] HÜNIG, S., and ERK, P., 1991, *Adv. Mater.*, **3**, 225.

[4] GOODINGS, E. P., 1976, *Chem. Soc. Rev.*, **5**, 95.

[5] WILLIAMS, D. J., 1984, *Angew. Chem.*, **96**, 637; 1984, *Angew. Chem. Int. Ed. Engl.*, **23**, 690.

[6] (a) RINGSDORF, H., SCHLARB, B., and VENZMER, J., 1988, *Angew. Chem.*, **100**, 117; 1988, *Angew. Chem. Int. Ed. Engl.*, **27**, 113. (b) HOGAN, J. L., IMRIE, C. T., and LUCKHURST, G. R., 1988, *Liq. Crystals*, **3**, 645. (c) ATTARD, G. C., GARNETT, S., HICKMAN, G. C., IMRIE, C. T., and TAYLOR, L., 1990, *Liq. Crystals*, **7**, 495.

[7] DEMUS, D., 1988, *Molec. Crystals liq. Crystals*, **165**, 45.

[8] PERCEC, V., and PUGH, C., 1989, *Side Chain Liquid Crystal Polymers*, edited by C. McArdle (Blackie & Son Ltd.), p. 30..

[9] KREUDER, W., RINGSDORF, H., HERMANN-SCHÖNHERR, O., and WENDORFF, J. H., 1987, *Angew. Chem.*, **99**, 1300; 1987, *Angew Chem. Int. Ed. Engl.*, **26**, 1249.

[10] CHIANG, L. Y., STOKES, J. P., SAFINYA, C. R., and BLOCH, A. N., 1985, *Molec. Crystals liq. Crystals*, **125**, 279.

[11] KEULEN, J. V., WARMERDAM, T. W., NOLTE, R. J. M., and DRENTH, W., 1987, *Recl. Trav. chim. Pays-Bas Belg.*, **106**, 534.

[12] BODEN, N., BUSCHBY, R. J., CLEMENTS, J., JESUDASON, M. V., KNOWLES, P. F., and WILLIAMS, G., 1988, *Chem. Phys. Lett.*, **152**, 94.

[13] SAEVA, F. D., REYNOLDS, G. A., and KASZCZUK, L., 1982, *J. Am. chem. Soc.*, **104**, 3524.

[14] DAVIDSON, P., LEVELUT, A. M., STRZELECKA, H., and GIONIS, V., 1983, *J. Phys. Lett. Paris*, **44**, 823.

[15] BENGS, H., EBERT, M., KARTHAUS, O., KOHNE, B., PRAEFCKE, K., RINGSDORF, H., WENDORFF, J. H., and WÜSTEFELD, R., 1990, *Adv. Mater.*, **2**, 141.

[16] GREEN, M. M., RINGSDORF, H., WAGNER, J., and WÜSTEFELD, R., 1990, *Angew. Chem.*, **102**, 1525; 1990, *Angew. Chem. Int. Ed. Engl.*, **29**, 1478.

[17] RINGSDORF, H., WÜSTEFELD, R., ZERTA, E., EBERT, M., and WENDORFF, J. H., 1989, *Angew. Chem.*, **101**, 934; 1989, *Angew. Chem. Int. Ed. Engl.*, **28**, 914.

[18] BAEHR, C., BENGS, H., EBERT, M., KARTHAUS, O., RINGSDORF, H., and WENDORFF, J. H., 1991, *Liquid Crystals*, **10**, 161.

[19] BENGS, H., RENKEL, R., RINGSDORF, H., BAEHR, C., EBERT, M., and WENDORFF, J. H., 1991, *Makromolek. Chem. rap. Commun.*, **12**, 439.

[20] NEWMAN, M. S., and JUNJAPPA, H., 1971, *J. org. Chem.*, **36**, 2606.

[21] BLOCK, P., and NEWMAN, M. S., 1973, *Organic Synthesis*, Vol. V (Wiley), p. 1031.

[22] KREUDER, W., and RINGSDORF, H., 1983, *Makromolek. Chem. rap. Commun.*, **4**, 807.

[23] KRANIG, W., HÜSER, B., SPIESS, H. W., KREUDER, W., RINGSDORF, H., and ZIMMERMANN, H., 1990, *Adv. Mater.*, **2**, 36.

[24] FUNHOFF, D., and CLOSS, F. (personal communication).

[25] (a) EBERT, M., 1990, Dissertation, TH Darmstadt. (b) TSUKRUK, V. V., SHILOV, V. V., and LIPATOV, YU. S., 1986, *Macromolecules*, **19**, 1308. (c) DURAN, R., GUILLON, D., GRAMAIN, P., and SKOULIOS, A., 1988, *J. Phys., Paris*, **49**, 121.

[26] PETKOV, V., and BAKALTCHEV, N., 1990, *J. appl. Cryst.*, **23**, 138.

[27] INSIGHT II, 1990, Biosym. Techn., CA 91121, San Diego.

[28] 1952, *International Tables for X-ray Crystallography* (Kynoch Press).

[29] LEVELUT, A. M., 1979, *J. Phys. Lett., Paris*, **40**, 81.

[30] KLUG, H., and ALEXANDER, L., 1954, *X-ray Diffraction Procedure* (Wiley).

[31] TSUKRUK, V., and SHILOV, V., 1990, *Structure of Polymeric Liquid Crystals* (Naukova Dumka).

[32] BAEHR, C., EBERT, M., FRICK, G., and WENDORFF, J. H., 1990, *Liq. Crystals*, **7**, 601.

[33] SPIESS, H. W., WERTH, M., BENGS, H., and RINGSDORF, H. (in preparation).